

## Hydrogen Evolution Catalyzed by Cobalt Diimine–Dioxime Complexes

Nicolas Kaeffer, Murielle Chavarot-Kerlidou, and Vincent Artero\*

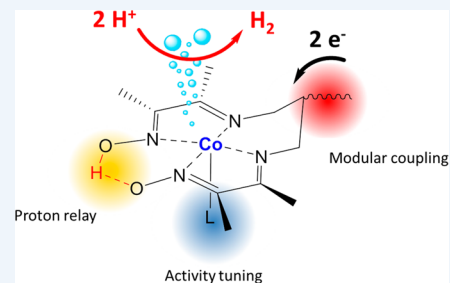
Laboratoire de Chimie Biologie des Métaux, Univ. Grenoble Alpes, CNRS, CEA Life Science Division, 17 rue des Martyrs, 38000 Grenoble, France

**CONSPECTUS:** Mimicking photosynthesis and producing solar fuels is an appealing way to store the huge amount of renewable energy from the sun in a durable and sustainable way. Hydrogen production through water splitting has been set as a first-ranking target for artificial photosynthesis. Pursuing that goal requires the development of efficient and stable catalytic systems, only based on earth abundant elements, for the reduction of protons from water to molecular hydrogen. Cobalt complexes based on glyoxime ligands, called cobaloximes, emerged 10 years ago as a first generation of such catalysts. They are now widely utilized for the construction of photocatalytic systems for hydrogen evolution.

In this Account, we describe our contribution to the development of a second generation of catalysts, cobalt diimine–dioxime complexes. While displaying similar catalytic activities as cobaloximes, these catalysts prove more stable against hydrolysis under strongly acidic conditions thanks to the tetradentate nature of the diimine–dioxime ligand. Importantly, H<sub>2</sub> evolution proceeds via proton-coupled electron transfer steps involving the oxime bridge as a protonation site, reproducing the mechanism at play in the active sites of hydrogenase enzymes. This feature allows H<sub>2</sub> to be evolved at modest overpotentials, that is, close to the thermodynamic equilibrium over a wide range of acid–base conditions in nonaqueous solutions.

Derivatization of the diimine–dioxime ligand at the hydrocarbon chain linking the two imine functions enables the covalent grafting of the complex onto electrode surfaces in a more convenient manner than for the parent bis-bidentate cobaloximes. Accordingly, we attached diimine–dioxime cobalt catalysts onto carbon nanotubes and demonstrated the catalytic activity of the resulting molecular-based electrode for hydrogen evolution from aqueous acetate buffer. The stability of immobilized catalysts was found to be orders of magnitude higher than that of catalysts in the bulk. It led us to evidence that these cobalt complexes, as cobaloximes and other cobalt salts do, decompose under turnover conditions where they are free in solution. Of note, this process generates in aqueous phosphate buffer a nanoparticulate film consisting of metallic cobalt coated with a cobalt-oxo/hydroxo-phosphate layer in contact with the electrolyte. This novel material, H<sub>2</sub>-CoCat, mediates H<sub>2</sub> evolution from neutral aqueous buffer at low overpotentials.

Finally, the potential of diimine–dioxime cobalt complexes for light-driven H<sub>2</sub> generation has been attested both in water/acetonitrile mixtures and in fully aqueous solutions. All together, these studies hold promise for the construction of molecular-based photoelectrodes for H<sub>2</sub> evolution and further integration in dye-sensitized photoelectrochemical cells (DS-PECs) able to achieve overall water splitting.



### INTRODUCTION

The amount of solar energy reaching the Earth exceeds our societal needs by several orders of magnitude.<sup>1</sup> However, worldwide energy demand does not correlate with the availability of sunlight. Trapping energy in chemical bonds, by producing fuels, is the only way to storing at the terawatt scale. Such a solution has already been massively implemented by photosynthetic organisms which use sunlight to sustain their metabolism and produce biomass. Mimicking this natural process to produce solar fuels is the founding principle of a large field of research called “artificial photosynthesis.”<sup>2</sup> Solar-driven water-splitting and production of molecular hydrogen has been set as a first target in this context, in line with the promises held by H<sub>2</sub> as an energy vector. A related key challenge is the finding of new efficient and robust catalysts based on earth abundant elements for the reduction of protons into H<sub>2</sub>.<sup>3</sup> To design such catalysts, inspiration naturally arises

from the dinuclear FeFe and NiFe active sites of hydrogenases (Figure 1),<sup>4</sup> the metallo-enzymes achieving H<sup>+</sup>/H<sub>2</sub> interconversion both at fast rate and close to the thermodynamic equilibrium. A number of promising catalytic systems derived from this approach.<sup>5</sup> Actually, mimics of another important enzyme, the cobalt-containing vitamin B<sub>12</sub> (Figure 1), also called cobalamin, proved among the most efficient molecular electrocatalysts for H<sub>2</sub> evolution. In its super-reduced state (B<sub>12</sub><sup>sr</sup>) featuring a Co<sup>I</sup> center, cobalamin is the most powerful nucleophile in nature.<sup>6</sup> Accordingly, cobalt bis-glyoximate complexes, largely developed by Schrauzer as B<sub>12</sub> mimics and known as cobaloximes (Figure 1),<sup>6</sup> can be protonated in their reduced form to yield hydridocobaloximes or tautomeric forms, the structure of which is still under investigation.<sup>7</sup> Such species

Received: February 2, 2015

Published: May 5, 2015

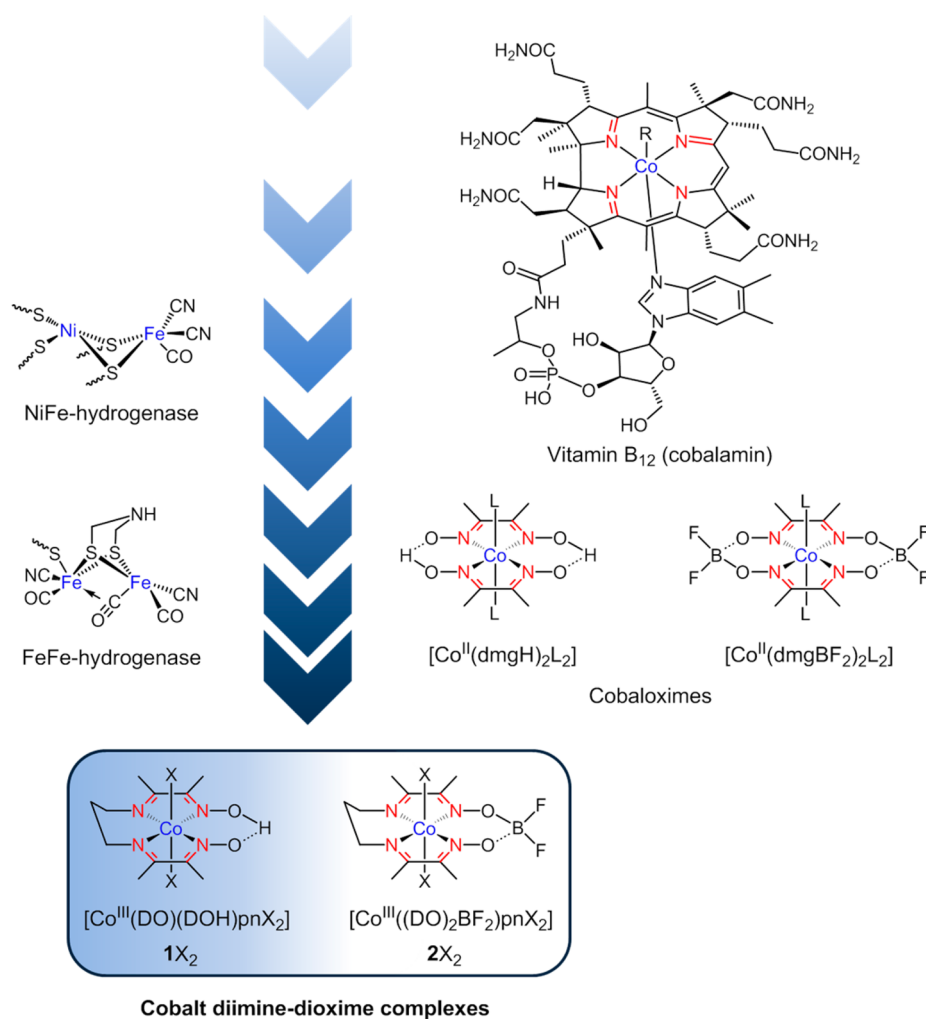


**Figure 1.** Structures of the active sites of NiFe and FeFe hydrogenases and of vitamin B<sub>12</sub> (R = H<sub>2</sub>O, CN<sup>-</sup>, CH<sub>3</sub>, adenosyl,...), proton-bridged and difluoroboryl-annulated cobaloximes (L = solvent (H<sub>2</sub>O, CH<sub>3</sub>CN, DMF)), and cobalt diimine–dioxime complexes 1X<sub>2</sub> and 2X<sub>2</sub> (X = Br, Cl,...).

actually turn to be the key intermediates in H<sub>2</sub> evolution catalyzed by this class of compounds.<sup>8</sup> Catalytic activity, initially reported in 1983 by Zissel and co-workers in the context of light-driven H<sub>2</sub> evolution,<sup>9</sup> was confirmed from 2005 by two independent electrochemical studies carried out in our laboratory<sup>10</sup> and in the one of Peters at Caltech.<sup>11</sup> Further studies involved, among others, the groups of Gray<sup>8b</sup> and Eisenberg.<sup>8c</sup> For now, cobaloximes appear as one of the most active series of molecular catalysts when considering turnover frequencies and overpotential requirement, as evidenced by a recent benchmarking study in nonaqueous solutions.<sup>12</sup> However, these compounds suffer from degradation in acidic solutions, which limits their stability under turnover conditions. This prompted us to investigate the reactivity of another class of B<sub>12</sub> mimics. Cobalt diimine–dioxime complexes (Figure 1), mainly developed by Marzilli and co-workers in the 1980s,<sup>13</sup> indeed contain single tetradentate equatorial ligands which are hardly displaced whereas hydrolysis of both oxime bridges in cobaloximes leads to the displacement (or exchange)<sup>14</sup> of both glyoxime ligands. In this Account, we highlight the potential of this second generation of cobalt catalysts for H<sub>2</sub> evolution as an opportunity to design molecular-engineered electrodes and light-driven systems working in aqueous media.

## ■ SYNTHESIS

Diimine–dioxime ligands are synthesized in one step through Schiff base condensation of butanedione–monoxime on diamine compounds. These ligands are abbreviated as (DOH)<sub>2</sub>xx where xx indicates the length of the hydrocarbon chain separating the two imine functions. Hence (DOH)<sub>2</sub>pn (Figure 1) corresponds to N<sup>2</sup>,N<sup>2'</sup>-propanediylbis-butan-2-imine-3-oxime. Metalation readily occurs when the ligand is reacted with a metallic salt.<sup>15</sup> Specifically, cobalt complexes rapidly react with oxygen from the air to yield octahedral Co<sup>III</sup> derivatives such as [Co(DO)(DOH)pnX<sub>2</sub>] (1X<sub>2</sub>, Figure 1), in which the diimine–dioxime ligand occupies all four equatorial positions. The oximate oxygen atoms are engaged in a hydrogen bond. The bridging proton can be replaced by a difluoroboryl group, as in [Co((DO)<sub>2</sub>BF<sub>2</sub>)pnX<sub>2</sub>] (2X<sub>2</sub>, Figure 1), through reaction with BF<sub>3</sub>·Et<sub>2</sub>O.

## ■ ELECTROCATALYTIC ACTIVITY FOR H<sub>2</sub> EVOLUTION

Black traces in Figure 2 correspond to the cyclic voltammograms (CVs) of 1Br<sub>2</sub> and 2Br<sub>2</sub> recorded in acetonitrile at a glassy carbon electrode.<sup>16</sup> Two quasi-reversible monoelectronic processes are observed corresponding to the stepwise reduction of the Co<sup>III</sup> complex to the Co<sup>II</sup> and Co<sup>I</sup> derivatives. X-ray

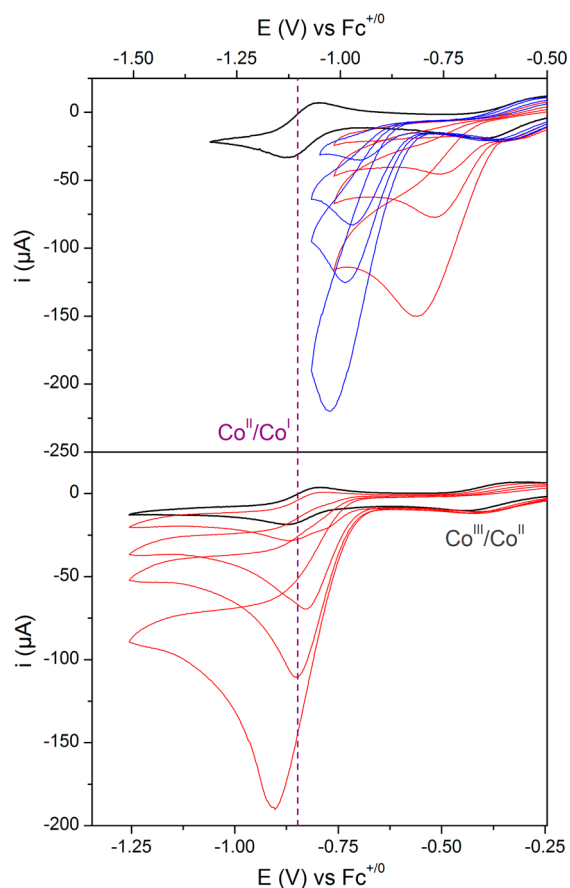


**Figure 2.** Cyclic voltammograms of  $1\text{Br}_2$  (top) and  $2\text{Br}_2$  (bottom) (1 mM, black traces) recorded in  $\text{CH}_3\text{CN}$  (0.1 M  $n\text{Bu}_4\text{NBF}_4$ ) at a glassy carbon electrode ( $100 \text{ mV}\cdot\text{s}^{-1}$ ) in the presence of *p*-cyanoanilinium tetrafluoroborate (red traces; 1, 3, 5, and 10 equiv) and anilinium tetrafluoroborate (blue traces; 1, 3, 5, and 10 equiv).

absorption spectroscopies have shown that halide ligands are fully displaced by acetonitrile in the reduced  $\text{Co}^{\text{II}}$  and  $\text{Co}^{\text{I}}$  states.<sup>17</sup> Upon reduction, the coordination number also decreases from 6 in the  $\text{Co}^{\text{III}}$  state to 5 in both the  $\text{Co}^{\text{II}}$  and  $\text{Co}^{\text{I}}$  state, a feature supported by DFT calculations.<sup>18</sup>

Electrocatalytic hydrogen evolution is evidenced in the CVs of  $1\text{Br}_2$  and  $2\text{Br}_2$  by the appearance of an irreversible wave that

raises in height with increasing concentrations of proton sources such as anilinium or *para*-cyanoanilinium.  $\text{H}_2$  production was quantified by gas chromatography coupled to coulometric monitoring, during bulk electrolysis experiments carried out at constant potential values corresponding to those of the electrocatalytic waves. In the case of the  $\text{BF}_2$ -annulated complex  $2\text{Br}_2$ , this electrocatalytic wave develops at potentials corresponding to the  $\text{Co}^{\text{II}}/\text{Co}^{\text{I}}$  process, in line with the behavior of cobaloximes (Figure 2).<sup>10,11</sup> By contrast, in the case of the H-bridged complex  $1\text{Br}_2$ , electrocatalytic  $\text{H}_2$  evolution occurs at potentials positively shifted with regard to the  $\text{Co}^{\text{II}}/\text{Co}^{\text{I}}$  couple. The extent of this shift depends on the strength of the acid used as proton source as shown in Figure 2. We hypothesized that proton transfer at the oxime bridge is involved in the rate-determining step of the catalytic reaction. To further support this hypothesis, we consequently carried out computational studies at the DFT level in collaboration with Field et al. at the Institute of Structural Biology in Grenoble.<sup>18a</sup> Figure 3 displays a part of the mechanistic scheme that resulted from calculations in good agreement, within methodological errors,<sup>19</sup> with electrochemically determined potentials of the redox processes (both measured and computed versus the  $\text{Fc}^+/\text{Fc}$  couple), and reproducing the electrocatalytic behavior of H-bridged diimine–dioxime complexes. The point of entry of the catalytic cycle is a  $\text{Co}^{\text{II}}$  derivative. A subsequent proton-coupled electron transfer process leads to a  $\text{Co}^{\text{I}}$  compound containing a protonated oxime bridge, which turns to be the initial active state, denoted as  $\text{Co}^{\text{I}}\text{LH}$ . Hammes-Schiffer and co-workers reached the same conclusion on the basis of similar DFT studies.<sup>18b</sup> The computed potential of the  $\text{Co}^{\text{II}}/\text{Co}^{\text{I}}\text{LH}$  couple appears significantly more positive than that of the  $\text{Co}^{\text{II}}/\text{Co}^{\text{I}}$  couple, consistent with the observed positive shift of the electrocatalytic potential. A second PCET step is then required to form a  $\text{Co}^{\text{II}}$ -hydride species bearing a protonated ligand,  $\text{Co}^{\text{II}}\text{HLH}$ . Finally,  $\text{H}_2$  is produced, either through external protonation or through an intramolecular mechanism that would reproduce the formation of a dihydrogen bond,<sup>20</sup> as suggested to occur at the active sites of hydrogenases.<sup>5a</sup> We have been able to locate a transition state for such an intramolecular process whose activation energy value is  $\sim 90 \text{ kJ mol}^{-1}$ , a value in agreement with other studies regarding  $\text{H}_2$ -evolving catalysts<sup>21</sup> or enzymes.<sup>22</sup> Formation of a  $\text{H}_2$ -bound species is suggested by theoretical computations. However,

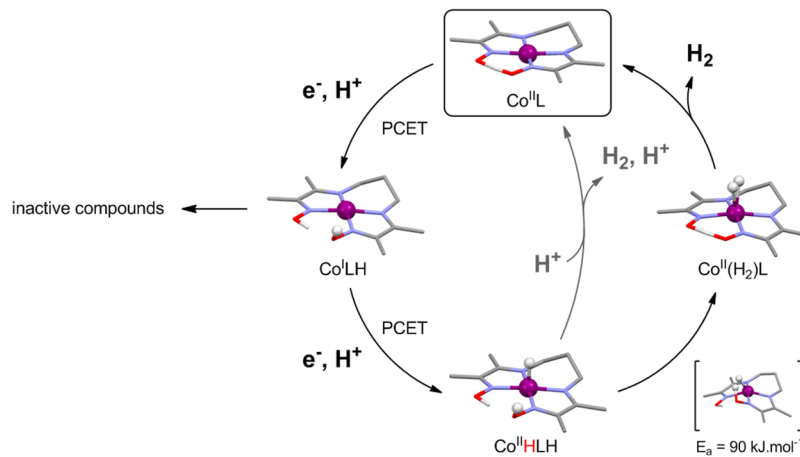


**Figure 3.** Possible pathways for catalytic hydrogen evolution, involving PCET processes, with DFT-optimized structures of the key intermediates. Axial ancillary ligands have been omitted for the sake of clarity.

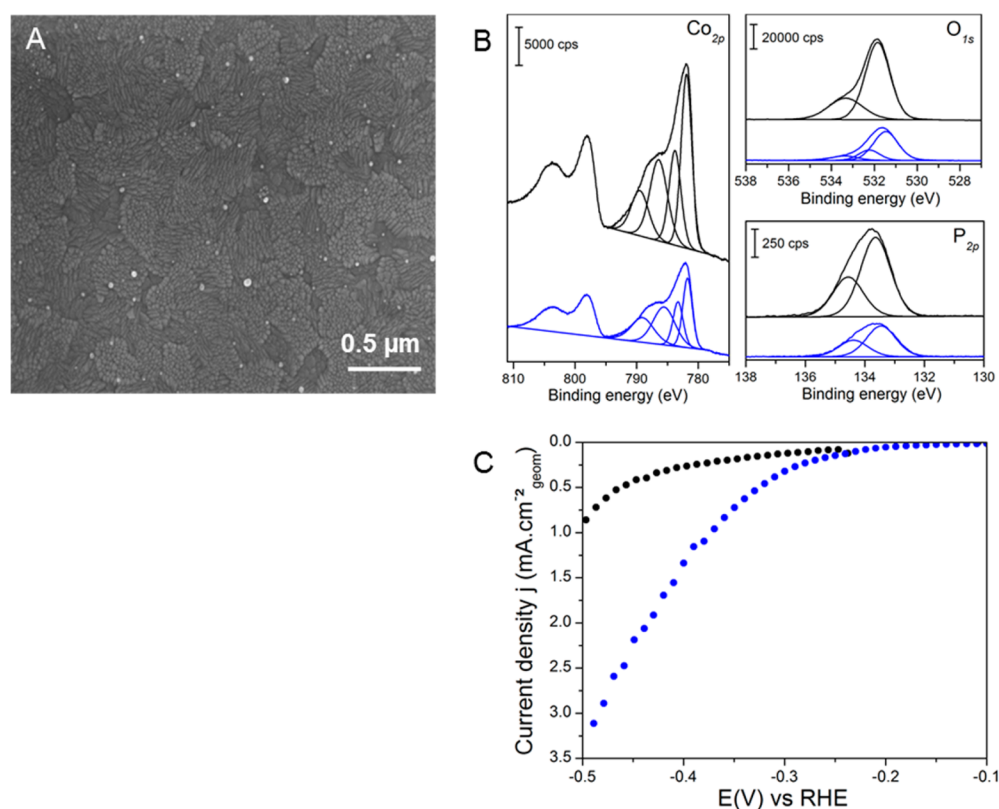


**Figure 4.** SEM image of an ITO electrode modified by electrolysis at  $-0.9$  V vs Ag/AgCl of a solution containing  $1\text{Cl}_2$  ( $0.5$  mM) in aqueous phosphate buffer ( $0.5$  M, pH 7) for 1 h ( $0.1\text{ C}\cdot\text{cm}^{-2}_{\text{geometric}}$ ) (A), XPS data ( $\text{Co}_{2p}$ ,  $\text{O}_{1s}$ , and  $\text{P}_{2p}$  cores) of a  $\text{H}_2$ -CoCat material deposited onto FTO substrate (blue traces) vs commercial  $\text{Co}_3(\text{PO}_4)_2\cdot x\text{H}_2\text{O}$  (black traces) (B), and polarization of a FTO electrode modified with  $\text{H}_2$ -CoCat (blue dots) compared with that of a Co foil electrode (black dots) in phosphate buffer ( $0.5$  M, pH 7) at  $0.05\text{ mV}\cdot\text{s}^{-1}$  (C). Reproduced with permission from ref 27. Copyright 2012 Nature Publishing Group.

**Table 1.**  $\text{p}K_a$ 's and Equilibrium Potentials of the  $\text{H}^+/\text{H}_2$  Couple in  $\text{CH}_3\text{CN}$  for Various Acids ( $10$  mM), Taking into Account Homoconjugation When Applicable,<sup>26</sup> Together with the Half-Wave Potentials of the Electrocatalytic Wave Corresponding to  $\text{H}_2$  Evolution Mediated by  $1\text{Br}_2$  (Data Reported in Refs 16 and 26)

	<i>p</i> -cyanoanilinium	tosic acid	anilinium	trifluoroacetic acid
$\text{p}K_a$	7.6	8.7	10.7	12.6
$E^\circ$ ( $\text{H}^+/\text{H}_2$ )	$-0.46$ V vs $\text{Fc}^{+/0}$	$-0.48$ V vs $\text{Fc}^{+/0}$	$-0.68$ V vs $\text{Fc}^{+/0}$	$-0.68$ V vs $\text{Fc}^{+/0}$
$E_{1/2}^{\text{cat}}$	$-0.68$ V vs $\text{Fc}^{+/0}$	$-0.73$ V vs $\text{Fc}^{+/0}$	$-0.92$ V vs $\text{Fc}^{+/0}$	$-0.96$ V vs $\text{Fc}^{+/0}$

given the fact that  $\text{H}_2$  elimination is entropically favored, it may not exist as a true intermediate in the catalytic mechanism.

Nonetheless, these calculations confirm that a  $\text{Co(II)}$ -hydride species is the active intermediate for  $\text{H}_2$  evolution, in agreement with the mechanism initially proposed by Eisenberg et al.,<sup>23</sup> and further supported by DFT studies by Muckerman and Fujita,<sup>24</sup> and Hammes-Schiffer and Solis<sup>25</sup> for parent cobaloximes. They also support a bridge-protonation pathway. Proton relays have already been shown crucial for promoting heterolytic  $\text{H}^+/\text{H}_2$  interconversion. The most popular examples are probably DuBois's nickel bisdiphosphine complexes containing basic amino sites in the second coordination sphere.<sup>5c</sup> Whether bridge protonation takes place in  $\text{H}_2$  evolution mediated by cobaloximes is unclear and still under investigation.<sup>7b,d,e</sup> In the present case, protonation of the oxime bridge allows diimine-dioxime complexes to adapt their electrocatalytic potential to the acid-base conditions of the medium, as shown in Table 1. Table 1 compares the potentials measured at half the catalytic wave and the equilibrium potential of the  $\text{H}^+/\text{H}_2$  couple in acetonitrile, computed from

tabulated values and taking into account the homoconjugation effect as previously reported.<sup>26</sup> From these data and in first approximation, it was possible to estimate the overpotential value at the middle of the catalytic wave (such an estimation is more accurate with S-shaped voltammograms recorded at rotating electrodes),<sup>26</sup> by subtracting the standard potential of the  $\text{H}^+/\text{H}_2$  couple from the measured value. It follows that the overpotential requirement for  $\text{H}_2$  evolution catalysis is kept within a  $220$ – $290$  mV window over a wide range of acid-base conditions, that is, in the presence of acids with  $\text{p}K_a$ 's ranging from  $7.6$  to  $12.6$ . To the best of our knowledge, such a behavior reproducing that of hydrogenases and platinum surfaces has never been reported for synthetic catalysts. In addition, these values compare well with those previously obtained for cobaloximes.<sup>10,11</sup> Current work in progress in our laboratory is devoted to the accurate determination of turnover frequencies, with the aim to establish "catalytic Tafel plots", displaying the relationship between turnover frequency and overpotential, for a rational benchmarking of the catalytic activity.<sup>12</sup>



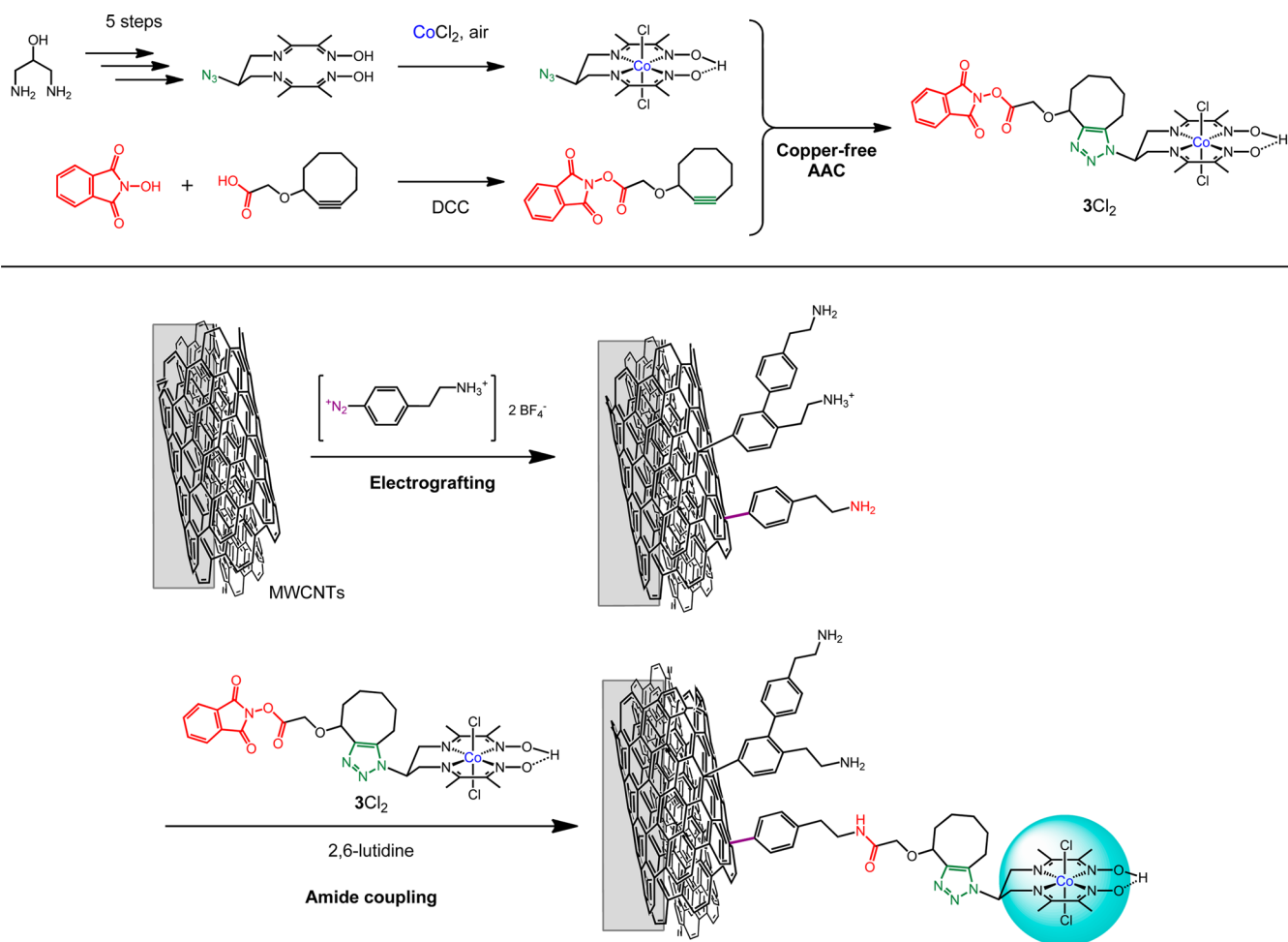


Figure 5. Synthetic strategy for the preparation of  $3\text{Cl}_2$ -functionalized MWCNTs electrodes (DCC = dicyclohexylcarbodiimide).

## ASSESSMENT OF CATALYTIC ACTIVITY IN AQUEOUS MEDIA

We found that diimine–dioxime complexes decompose under aqueous catalytic conditions. Actually, in pH 7 aqueous phosphate buffer they experience an electroreductive transformation into a nanoparticulate material which is deposited on the electrode as confirmed by SEM analysis (Figure 4A).<sup>27</sup> Small nanoparticles with average diameter of 10 nm (Figure 4A) are initially formed. Upon prolonged deposition time or when reduction is carried out at a more negative potential, an  $\sim 2\ \mu\text{m}$  thick film made of larger particles (100 nm) is obtained. The same coating can be obtained starting from simple cobalt salts. On the basis of advanced spectroscopic measurements (XPS; Figure 4B, EDX, EXAFS, and XANES), we could show that this novel material, called  $\text{H}_2\text{-CoCat}$ , consists of metallic cobalt coated with a cobalt-oxo/hydroxo/phosphate layer in contact with the electrolyte. Interestingly,  $\text{H}_2\text{-CoCat}$  mediates  $\text{H}_2$  evolution from neutral aqueous buffer with onset potential, that is, the potential at which we could analytically detect  $\text{H}_2$  evolution using continuous-flow gas chromatography, of 50 mV vs RHE (Figure 4C). Remarkably, it can be converted upon anodic equilibration into the cobalt-oxide film catalyzing  $\text{O}_2$  evolution described by Nocera et al.<sup>28</sup> The switch between the two catalytic forms is fully reversible and corresponds to a local interconversion between two morphologies and compositions at the surface of the electrode.

This raises the general and important question of distinguishing true homogeneous catalysis by metal complexes from heterogeneous catalysis by metal or metal-oxide particles derived from in situ transformations. This situation, much more prevalent than currently appreciated, sometimes hard to detect and quite ubiquitous in catalysis, has been recently reviewed in the context of electro- or photochemical processes.<sup>29</sup> As an example,  $\text{H}_3\text{PO}_4/\text{H}_2\text{PO}_4^-$  aqueous solution (pH 2.2) was previously reported suitable for the benchmarking of the catalytic activity for  $\text{H}_2$  evolution of molecular cobalt catalysts including  $1(\text{H}_2\text{O})^{2+}$ .<sup>30a</sup> However, recent investigations in our laboratory evidenced that decomposition occurs under these conditions, accompanied by the deposition of an electrocatalytically active coating at the electrode.<sup>30b</sup> Similar observations have also been made for cobalt complexes in nonaqueous media in the presence of strong acids.<sup>31</sup>

## MOLECULAR-BASED ELECTRODE MATERIALS

The results described above may seem disappointing, at least in the context of molecular chemistry. Ligand design allows for a fine-tuning of the catalytic properties, but the inherent fragility of the resulting catalysts, when exposed to reducing/oxidizing and/or hydrolytic conditions, may condemn such an approach in the context of photoelectrochemical water splitting. In other words, is it worth developing molecular catalysts if they transform under turnover conditions into catalytically active species that can alternatively be obtained from simple metal

salts? The answer is “yes”, since we could evidence that immobilization onto electrode surface is a very efficient way to stabilize such molecular catalysts and avoid their degradation/transformation under catalytic conditions. To achieve this goal, we functionalized the hydrocarbon chain bridging the two imine functions to create a covalent link between these catalysts and multiwall carbon nanotubes (MWCNTs) used as electrode material. We first prepared an azido derivative starting from 2-hydroxy-1,3-diaminopropane (Figure 5).<sup>32</sup> Alternatively, malonic synthesis strategies proved fruitful to generate a series of ligands derivatized with different functional groups.<sup>33</sup> In our case, azide–alkyne coupling (AAC) allowed preparation of  $3\text{Cl}_2$  (Figure 5) containing a terminal activated ester group. For that purpose, we used a strained cyclooctyne precursor enabling the use of copper-free AAC conditions<sup>34</sup> and thus avoiding substitution of copper for cobalt in the complex. In parallel, MWCNTs, deposited as a mat, were decorated with amino functions through the electroreduction of 4-(2-aminoethyl)-benzene diazonium. This results in the coating of the electrode with a film of aminoethylphenylene oligomers as represented in Figure 5.<sup>35</sup> Finally  $3\text{Cl}_2$  was covalently, thus durably, anchored on MWCNTs through the formation of amide linkages, as confirmed by XPS.

Cyclic voltammograms measured on the modified electrode displayed two redox systems corresponding to the  $\text{Co}^{\text{III}}/\text{Co}^{\text{II}}$  and  $\text{Co}^{\text{II}}/\text{Co}^{\text{I}}$  couples (Figure 6) assigned by analogy with  $3\text{Cl}_2$ .

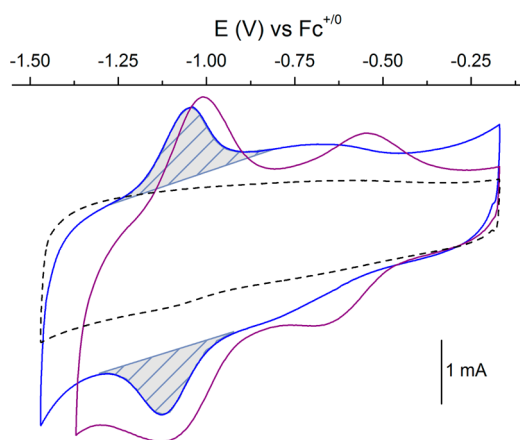


**Figure 6.** Cyclic voltammogram of  $3\text{Cl}_2$  recorded in  $\text{CH}_3\text{CN}$  (0.1 M  $n\text{Bu}_4\text{NBF}_4$ ) at a MWCNT electrode (purple trace) and cyclic voltammogram of a  $3\text{Cl}_2$ -functionalized MWCNTs electrode (blue trace) recorded in  $\text{CH}_3\text{CN}$  (0.1 M  $\text{Et}_4\text{NCl}$ ). The response of the unmodified MWCNTs electrode is represented with a dashed black trace. Scan rate:  $100 \text{ mV}\cdot\text{s}^{-1}$ .

The first system is ill-defined, but the  $\text{Co}^{\text{II}}/\text{Co}^{\text{I}}$  wave is reversible with peak intensities directly proportional to scan rate, confirming covalent immobilization of the cobalt complexes on the electrode surface. Surface concentrations as high as  $4.5 \text{ nmol}\cdot\text{cm}^{-2}$  could be determined from the integration of this mono-electronic system.

The resulting material proved active for electrocatalytic  $\text{H}_2$  generation at relatively low overpotentials from pure aqueous solutions ranging from pH 2.2 to 5, whereas no catalytic activity could be detected in pH 7 phosphate buffer solutions.<sup>36</sup> The onset potential for  $\text{H}_2$  evolution was found to be 350 mV vs RHE in pH 4.5 acetate buffer (Figure 7).<sup>32</sup> This material is also remarkably stable, allowing extensive cycling without degradation. This is underlined by a 7 h electrolysis experiment, during

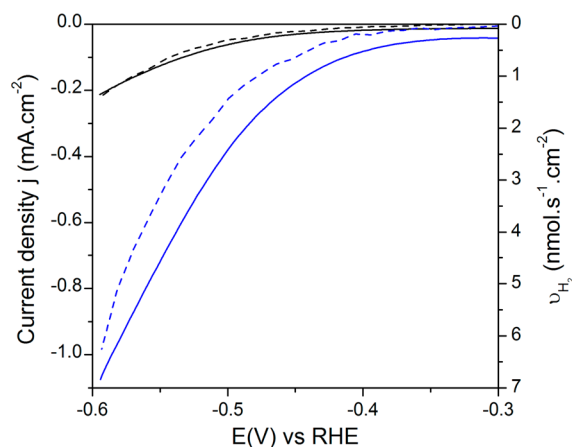


**Figure 7.** Linear sweep voltammograms (solid traces; left scale) of a  $3\text{Cl}_2$ -functionalized MWCNTs electrode (blue trace) compared to unmodified MWCNTs material (black trace) in a pH 4.5 acetate buffer (0.1 M) recorded at  $0.1 \text{ mV}\cdot\text{s}^{-1}$  with simultaneous monitoring of  $\text{H}_2$  production rate (dashed traces; right scale) using constant-flow continuous GC measurements.

which each immobilized cobalt center achieves more than 50 000 turnovers without significant deactivation. Electrochemical and XPS measurements confirmed preservation of the molecular structure (except for axial ligands that are rapidly exchanged in reduced states)<sup>17</sup> of the grafted complex after catalytic turnover. SEM was also used to exclude the formation of any deposit, such as the  $\text{H}_2$ -CoCat material,<sup>27</sup> at the surface of MWCNTs.

Previous studies of  $1\text{Br}_2$  solubilized in nonaqueous media showed significant degradation after 50 turnovers.<sup>16</sup> This clearly indicates that grafting provides a largely increased protection of these cobalt catalysts against modification during extensive cycling. A similar example has been reported by our group with DuBois' nickel bisdiphosphine catalysts. Once immobilized on carbon nanotubes, they can turn over more than 100 000 times without loss of activity or formation of heterogeneous active metal species.<sup>37a,b</sup> Though no detailed “postmortem” analysis has been reported for cobaloxime or cobalt diimine–dioxime catalysts yet, a recent work on related diimine–dipyridine metal complexes<sup>38</sup> showed insightful details on possible deactivation pathways. Reduction at the metal site may generate transient carbon-based  $\alpha$ -imino radical species subjected to reductive homocoupling, that finally yields dimeric complexes with new metal coordination spheres likely not suitable for catalysis. Our hypothesis is that once grafted onto electrode materials the molecular complexes are isolated one from each other and cannot react in such bimolecular manner. Another mechanism for deactivation includes ligand hydrogenation through hydride transfer from the  $\text{Co}^{\text{III}}\text{HL}$  species, either directly formed from the  $\text{Co}^{\text{I}}$  state or through isomerism of the  $\text{Co}^{\text{I}}\text{LH}$  species (Figure 3).<sup>39</sup> For complexes grafted onto electrodes, immediate reduction of this species is likely to compete with hydride transfer and to form the catalytically competent  $\text{Co}^{\text{II}}$ -hydride species, resulting in enhanced activity and stability.

We note however that covalent immobilization of a catalyst is not always as straightforward as a way to generate efficient electrocatalytic materials. This point arises from, at least, two reasons. First, the linker introduced between the catalytic moiety and the surface often acts as an insulator, which results in the requirement of increased overpotentials for catalysis to occur.<sup>3,40</sup> In the course of a long-standing and fruitful

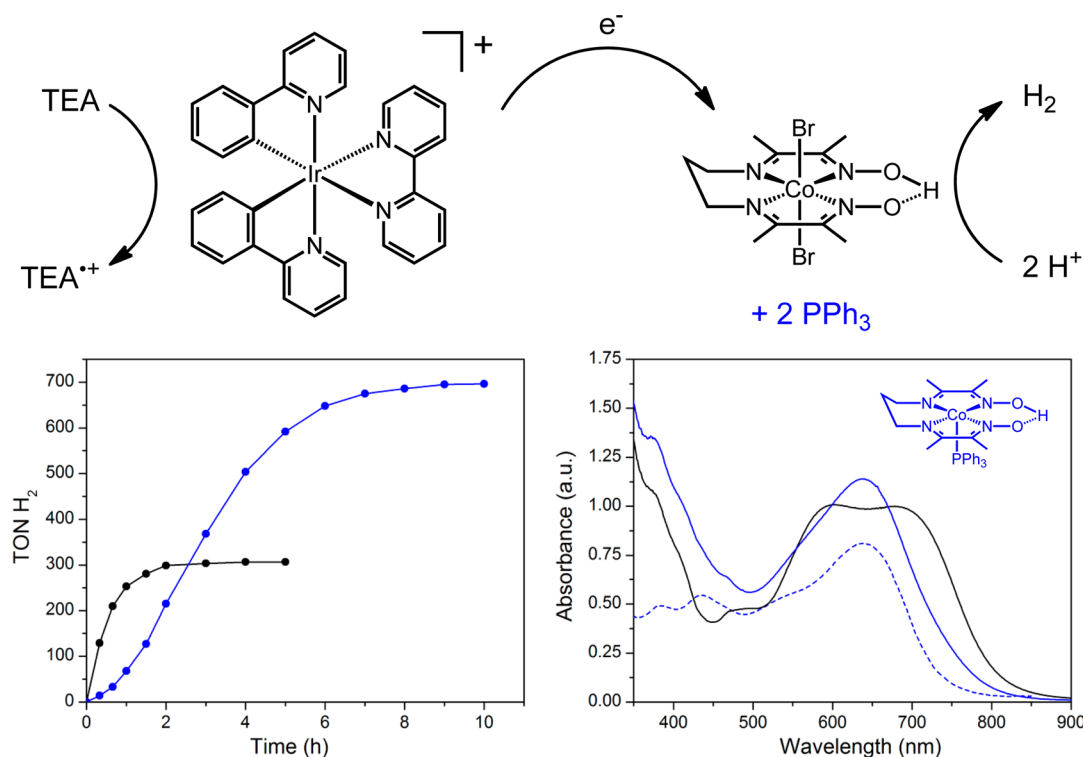


**Figure 8.** Photocatalytic system based on  $1\text{Br}_2$  (top),  $\text{H}_2$  evolution versus time (bottom left), and spectroscopic signature of the resting state (bottom right) during continuous irradiation in the absence (black traces) and the presence (blue traces) of 2 equiv of  $\text{PPh}_3$ . The dashed blue trace shows the spectrum of authentic  $[\text{Co}(\text{DO})(\text{DOH})\text{pn}(\text{PPh}_3)]$ .

collaboration with Jusselme, Palacin, and co-workers from the Matter Science Division of CEA (Saclay, France),<sup>27,32,35,37</sup> we could show that, when performed onto MWCNTs, the electroreduction of diazonium salts provides a quite unique way to graft a significant amount of redox probes on the electrode surface without introducing such electron transfer barrier.<sup>35b</sup> Second, the structure of a molecular catalyst is significantly reorganized on completion of the catalytic cycle. This statement is particularly true for redox catalysts transitioning through various oxidation states. The immobilization mode must thus enable easy conformational changes. Grafting of diimine–dioxime complexes onto oxide surfaces has been described by Peters and Berben,<sup>41</sup> and Reisner and co-workers.<sup>33a,42</sup> However, these immobilization modes, involving two anchoring groups, do not allow for  $\text{H}_2$  evolution catalysis to occur at significant rate, which probably originates from constraints generated at the cobalt center upon grafting.

## ■ PHOTOCHEMICAL SYSTEMS

Cobalt diimine–dioxime catalysts also proved to be active for  $\text{H}_2$  evolution under light-driven conditions through their association with molecular Ru-, Ir-, or Re-based photosensitizers. Such homogeneous systems rely on sacrificial electron donors such as triethanolamine, triethylamine (TEA), or ascorbic acid. In the context of a collaboration with the group of Wang and Sun at Dalian Institute of Technology (China), we assessed the photocatalytic activity of  $1\text{Br}_2$  in mixed  $\text{H}_2\text{O}/\text{CH}_3\text{CN}$  conditions in the presence of TEA and a cyclometalated iridium-based photosensitizer.<sup>43</sup> Turnover numbers (TON) as high as 300 could be obtained after 4 h of visible light irradiation. Under the same conditions, the  $\text{BF}_2$ -annulated complex  $2\text{Br}_2$  only led to 50 TON, consistent with the inability of this complex to be protonated at the oxime

bridge. The addition of triphenylphosphine resulted in a significant increase of the stability of the system with up to 700 TON achieved within 10 h (Figure 8). Phosphine ligands are known to stabilize low oxidation states of cobalt complexes that are the key intermediates in the  $\text{H}_2$  evolution mechanism. Indeed, stabilization of the  $\text{Co}^{\text{I}}$  state of  $1\text{Br}_2$  by coordination of  $\text{PPh}_3$  has been confirmed by cyclic voltammetry measurements with a  $\sim 280$  mV anodic shift of the electrochemical potential of the  $\text{Co}^{\text{II}}/\text{Co}^{\text{I}}$  couple. In order to get more information on the reduced species generated during photocatalysis, we monitored the reaction using UV–vis spectroscopy: starting from the  $\text{Co}^{\text{III}}$  complex, irradiation leads after 10–20 s to a first absorption band at 472 nm, characteristic of a  $\text{Co}^{\text{II}}$  species. When  $\text{PPh}_3$  is present in solution, a second band at 638 nm then appears after 70 s, corresponding to the exact signature of the  $\text{Co}^{\text{I}}$  complex  $[\text{Co}(\text{DO})(\text{DOH})\text{pn}(\text{PPh}_3)]$  (Figure 8). By contrast, in the absence of  $\text{PPh}_3$ , the resting state of the catalyst displayed another signature, characterized by two new bands centered at 602 and 678 nm. Similar spectroscopic signatures have been reported for reduced cobaloxime  $[\text{Co}(\text{dmgBF}_2)_2(\text{H}_2\text{O})_2]$ <sup>7e,11b,23,44</sup> and have been assigned to a spectroscopic  $\text{Co}^{\text{I}}$  state, a statement supported by ab initio calculations.<sup>45</sup> However, a similar spectrum has also been calculated for a  $\text{Co}^{\text{II}}\text{–H}$  intermediate.<sup>24</sup> While more studies are still needed to fully characterize these intermediates, it seems that coordination of the  $\pi$ -acceptor phosphine ligand stabilizes the system by preventing side reactions, such as the above-mentioned hydride transfer processes,<sup>39b,c</sup> to occur. Similarly, a derivative of  $1\text{Br}_2$  containing a pendant methylpyridine ligand<sup>33b</sup> showed increased activity under photochemical conditions.<sup>46</sup> These results highlight the relevance of ligand tuning for the optimization of such systems.



Cobalt diimine–dioxime catalysts so far display lower activity under light driven conditions as compared to parent cobaloximes.<sup>8a,c</sup> They however prove quite versatile as H<sub>2</sub> evolution catalysts as far as the reaction conditions are concerned: they function in fully organic solutions<sup>47</sup> as well as in fully aqueous conditions.<sup>46,48</sup> Not surprisingly, the optimal acid/base conditions in terms of activity in water (up to 90 TON) correspond to a pH of 4,<sup>48a</sup> thus matching the optimal value determined for the molecular-based cathode material containing the same cobalt diimine–dioxime catalytic moiety.<sup>32</sup>

## SUMMARY AND OUTLOOK

In the past 5 years, we have developed cobalt diimine–dioxime complexes as molecular catalysts for H<sub>2</sub> evolution. The tetradentate nature of the diimine–dioxime ligand warrants stability against hydrolysis, while letting an oxime bridge available to act as a proton relay. In addition, derivatization of this ligand at the hydrocarbon chain bridging the two imine functions enables its coupling with a surface, or possibly a photosensitizer, in a much more convenient manner than for the parent cobaloximes. Cobalt diimine–dioxime catalysts finally prove active for H<sub>2</sub> evolution in fully aqueous conditions both after immobilization onto electrode materials and in light-driven homogeneous conditions. These two properties hold promise for the construction of molecular-based photocathodes as key components of dye-sensitized photoelectrochemical cells.

## AUTHOR INFORMATION

### Corresponding Author

\*E-mail: vincent.artero@cea.fr.

### Notes

The authors declare no competing financial interest.

### Biographies

**Nicolas Kaefffer** received both a Chimie ParisTech engineer diploma and a master level in molecular chemistry from the Université Pierre et Marie Curie (Paris) in 2012. Since there, he works as a graduate student in CEA-Grenoble on the construction of molecular cathodes and photocathodes for hydrogen evolution based on cobalt diimine–dioxime complexes, under the supervision of Dr. Vincent Artero.

**Murielle Chavarot-Kerlidou** studied organic chemistry at the University of Grenoble (Ph.D. 1998) and obtained a CNRS position (2002) to develop organometallic chemistry in Paris, from where she moved in 2009 to join CEA-Grenoble and work on hydrogen photoproduction.

**Vincent Artero** graduated from the Ecole Normale Supérieure (Ulm) and studied inorganic chemistry at the University Pierre et Marie Curie in Paris (Ph.D. 2000). He moved to the CEA center in Grenoble (Life Science Division) in 2001 to develop bioinspired chemistry related to hydrogen production and artificial photosynthesis. He received the “Grand Prix Mergier-Bourdeix de l’Académie des Sciences” (2011) and was granted in 2012 with a Starting Grant from the European Research Council (ERC).

## ACKNOWLEDGMENTS

We thank Pierre-André Jacques, Eugen S. Andreiadis, Saioa Cobo, Jennifer Fize, Marc Fontecave, and our collaborators for discussion and important contributions to cobalt diimine–dioxime chemistry. This work was supported by the French National Research Agency (Labex program, ARCANÉ, ANR-

11-LABX-0003-01), the European Research Council under the European Union’s Seventh Framework Programme (FP/2007-2013)/ERC Grant Agreement No. 306398, and the Life Science Division of CEA (2011 DSV-Energy program).

## REFERENCES

- (1) Sherman, B.; Vaughn, M.; Bergkamp, J.; Gust, D.; Moore, A.; Moore, T. Evolution of reaction center mimics to systems capable of generating solar fuel. *Photosynth. Res.* **2014**, *120*, 59–70.
- (2) Andreiadis, E. S.; Chavarot-Kerlidou, M.; Fontecave, M.; Artero, V. Artificial Photosynthesis: From Molecular Catalysts for Light-driven Water Splitting to Photoelectrochemical Cells. *Photochem. Photobiol.* **2011**, *87*, 946–964.
- (3) Artero, V.; Fontecave, M. Some general principles for designing electrocatalysts with hydrogenase activity. *Coord. Chem. Rev.* **2005**, *249*, 1518–1535.
- (4) Lubitz, W.; Ogata, H.; Rüdiger, O.; Reijerse, E. Hydrogenases. *Chem. Rev.* **2014**, *114*, 4081–4148.
- (5) (a) Simmons, T. R.; Berggren, G.; Bacchi, M.; Fontecave, M.; Artero, V. Mimicking hydrogenases: From biomimetics to artificial enzymes. *Coord. Chem. Rev.* **2014**, *270–271*, 127–150. (b) Canaguier, S.; Artero, V.; Fontecave, M. Modelling NiFe hydrogenases: nickel-based electrocatalysts for hydrogen production. *Dalton Trans.* **2008**, *39*, 315–325. (c) DuBois, D. L. Development of Molecular Electrocatalysts for Energy Storage. *Inorg. Chem.* **2014**, *53*, 3935–3960.
- (6) Schrauzer, G. N. Organocobalt chemistry of vitamin B<sub>12</sub> model compounds (cobaloximes). *Acc. Chem. Res.* **1968**, *1*, 97–103.
- (7) (a) Schrauzer, G. N.; Holland, R. J. Hydridocobaloximes. *J. Am. Chem. Soc.* **1971**, *93*, 1505–1506. (b) Bhattacharjee, A.; Chavarot-Kerlidou, M.; Andreiadis, E. S.; Fontecave, M.; Field, M. J.; Artero, V. Combined Experimental-Theoretical Characterization of the Hydrido-Cobaloxime [HCo(dmgH)<sub>2</sub>(P<sup>n</sup>Bu<sub>3</sub>)]. *Inorg. Chem.* **2012**, *51*, 7087–7093. (c) Chao, T. H.; Espenson, J. H. Mechanism of Hydrogen Evolution from Hydridocobaloxime. *J. Am. Chem. Soc.* **1978**, *100*, 129–133. (d) Lacy, D. C.; Roberts, G. M.; Peters, J. C. The Cobalt Hydride that Never Was: Revisiting Schrauzer’s “Hydridocobaloxime”. *J. Am. Chem. Soc.* **2015**, *137*, 4860–4864. (e) Estes, D. P.; Grills, D. C.; Norton, J. R. The Reaction of Cobaloximes with Hydrogen: Products and Thermodynamics. *J. Am. Chem. Soc.* **2014**, *136*, 17362–17365.
- (8) (a) Artero, V.; Chavarot-Kerlidou, M.; Fontecave, M. Splitting water with cobalt. *Angew. Chem., Int. Ed.* **2011**, *50*, 7238–7266. (b) Dempsey, J. L.; Brunschwig, B. S.; Winkler, J. R.; Gray, H. B. Hydrogen Evolution Catalyzed by Cobaloximes. *Acc. Chem. Res.* **2009**, *42*, 1995–2004. (c) Eckenhoff, W. T.; McNamara, W. R.; Du, P.; Eisenberg, R. Cobalt complexes as artificial hydrogenases for the reductive side of water splitting. *Biochim. Biophys. Acta* **2013**, *1827*, 958–973.
- (9) Hawecker, J.; Lehn, J. M.; Zissel, R. Efficient Homogeneous Photochemical Hydrogen Generation and Water Reduction Mediated by Cobaloxime or Macrocyclic Cobalt Complexes. *New J. Chem.* **1983**, *7*, 271–277.
- (10) (a) Razavet, M.; Artero, V.; Fontecave, M. Proton electroreduction catalyzed by cobaloximes: Functional models for hydrogenases. *Inorg. Chem.* **2005**, *44*, 4786–4795. (b) Baffert, C.; Artero, V.; Fontecave, M. Cobaloximes as functional models for hydrogenases. 2. proton electroreduction catalyzed by difluoroborylbis-(dimethylglyoximate)cobalt(II) complexes in organic media. *Inorg. Chem.* **2007**, *46*, 1817–1824.
- (11) (a) Hu, X. L.; Cossairt, B. M.; Brunschwig, B. S.; Lewis, N. S.; Peters, J. C. Electrocatalytic hydrogen evolution by cobalt difluoroboryl-diglyoximate complexes. *Chem. Commun.* **2005**, *45*, 4723–4725. (b) Hu, X.; Brunschwig, B. S.; Peters, J. C. Electrocatalytic hydrogen evolution at low overpotentials by cobalt macrocyclic glyoxime and tetraimine complexes. *J. Am. Chem. Soc.* **2007**, *129*, 8988–8998.



- (12) Artero, V.; Saveant, J.-M. Toward the rational benchmarking of homogeneous H<sub>2</sub>-evolving catalysts. *Energy Environ. Sci.* **2014**, *7*, 3808–3814.
- (13) Seeber, R.; Parker, W. O.; Marzilli, P. A.; Marzilli, L. G. Electrochemical Synthesis of Costa-Type Cobalt Complexes. *Organometallics* **1989**, *8*, 2377–2381.
- (14) McCormick, T. M.; Han, Z. J.; Weinberg, D. J.; Brennessel, W. W.; Holland, P. L.; Eisenberg, R. Impact of Ligand Exchange in Hydrogen Production from Cobaloxime-Containing Photocatalytic Systems. *Inorg. Chem.* **2011**, *50*, 10660–10666.
- (15) Costa, G.; Mestroni, G.; de Savognani, E. *Inorg. Chim. Acta* **1969**, *3*, 323–328.
- (16) Jacques, P.-A.; Artero, V.; Pécaut, J.; Fontecave, M. Cobalt and nickel diimine–dioxime complexes as molecular electrocatalysts for hydrogen evolution with low overvoltages. *Proc. Natl. Acad. Sci. U.S.A.* **2009**, *106*, 20627–20632.
- (17) Giorgetti, M.; Berrettoni, M.; Ascone, I.; Zamponi, S.; Seeber, R.; Marassi, R. X-ray absorption spectroscopy study on the electrochemical reduction of Co((DO)(DOH)(pn))Br<sub>2</sub>. *Electrochim. Acta* **2000**, *45*, 4475–4482.
- (18) (a) Bhattacharjee, A.; Andreiadis, E. S.; Chavarot-Kerlidou, M.; Fontecave, M.; Field, M. J.; Artero, V. A Computational Study of the Mechanism of Hydrogen Evolution by Cobalt (Diimine-Dioxime) Catalysts. *Chem.—Eur. J.* **2013**, *19*, 15166–15174. (b) Solis, B. H.; Yu, Y.; Hammes-Schiffer, S. Effects of Ligand Modification and Protonation on Metal Oxime Hydrogen Evolution Electrocatalysts. *Inorg. Chem.* **2013**, *52*, 6994–6999.
- (19) Roy, L. E.; Jakubikova, E.; Guthrie, M. G.; Batista, E. R. Calculation of One-Electron Redox Potentials Revisited. Is It Possible to Calculate Accurate Potentials with Density Functional Methods? *J. Phys. Chem. A* **2009**, *113*, 6745–6750.
- (20) Niu, S.; Hall, N. B. Modeling the active sites in metalloenzymes 5. The heterolytic bond cleavage of H<sub>2</sub> in the [NiFe] hydrogenase of *Desulfovibrio gigas* by a nucleophilic addition mechanism. *Inorg. Chem.* **2001**, *40*, 6201–6203.
- (21) Sundstrom, E. J.; Yang, X.; Thoi, V. S.; Karunadasa, H. I.; Chang, C. J.; Long, J. R.; Head-Gordon, M. Computational and Experimental Study of the Mechanism of Hydrogen Generation from Water by a Molecular Molybdenum-Oxo Electrocatalyst. *J. Am. Chem. Soc.* **2012**, *134*, 5233–5242.
- (22) Ridder, L.; Mulholland, A. J.; Vervoort, J.; Rietjens, I. M. C. M. Correlation of Calculated Activation Energies with Experimental Rate Constants for an Enzyme Catalyzed Aromatic Hydroxylation. *J. Am. Chem. Soc.* **1998**, *120*, 7641–7642.
- (23) Du, P. W.; Schneider, J.; Luo, G. G.; Brennessel, W. W.; Eisenberg, R. Visible Light-Driven Hydrogen Production from Aqueous Protons Catalyzed by Molecular Cobaloxime Catalysts. *Inorg. Chem.* **2009**, *48*, 4952–4962.
- (24) Muckerman, J. T.; Fujita, E. Theoretical Studies of the Mechanism of Catalytic Hydrogen Production by a Cobaloxime. *Chem. Commun.* **2011**, *47*, 12456–12458.
- (25) Solis, B. H.; Hammes-Schiffer, S. Theoretical Analysis of Mechanistic Pathways for Hydrogen Evolution Catalyzed by Cobaloximes. *Inorg. Chem.* **2011**, *50*, 11252–11262.
- (26) Fourmond, V.; Jacques, P. A.; Fontecave, M.; Artero, V. H<sub>2</sub> Evolution and Molecular Electrocatalysts: Determination of Overpotentials and Effect of Homoconjugation. *Inorg. Chem.* **2010**, *49*, 10338–10347.
- (27) Cobo, S.; Heidkamp, J.; Jacques, P.-A.; Fize, J.; Fourmond, V.; Guetaz, L.; Jusselme, B.; Ivanova, V.; Dau, H.; Palacin, S.; Fontecave, M.; Artero, V. A Janus cobalt-based catalytic material for electro-splitting of water. *Nat. Mater.* **2012**, *11*, 802–807.
- (28) Kanan, M. W.; Surendranath, Y.; Nocera, D. G. Cobalt-phosphate oxygen-evolving compound. *Chem. Soc. Rev.* **2009**, *38*, 109–114.
- (29) Artero, V.; Fontecave, M. Solar fuels generation and molecular systems: is it homogeneous or heterogeneous catalysis? *Chem. Soc. Rev.* **2013**, *42*, 2338–2356.
- (30) (a) McCrory, C. C. L.; Uyeda, C.; Peters, J. C. Electrocatalytic Hydrogen Evolution in Acidic Water with Molecular Cobalt Tetraazamacrocycles. *J. Am. Chem. Soc.* **2012**, *134*, 3164–3170. (b) Kaeffer, N.; Morozan, A.; Artero, V. *Unpublished data*.
- (31) (a) Anxolabéhère-Mallart, E.; Costentin, C.; Fournier, M.; Nowak, S.; Robert, M.; Savéant, J. M. Boron-Capped Tris(glyoximate) Cobalt Clathrochelate as a Precursor for the Electrodeposition of Nanoparticles Catalyzing H<sub>2</sub> Evolution in Water. *J. Am. Chem. Soc.* **2012**, *134*, 6104–6107. (b) Anxolabéhère-Mallart, E.; Costentin, C.; Fournier, M.; Robert, M. Cobalt-Bisglyoximate Diphenyl Complex as a Precatalyst for Electrocatalytic H<sub>2</sub> Evolution. *J. Phys. Chem. C* **2014**, *118*, 13377–13381.
- (32) Andreiadis, E. S.; Jacques, P.-A.; Tran, P. D.; Leyris, A.; Chavarot-Kerlidou, M.; Jusselme, B.; Matheron, M.; Pécaut, J.; Palacin, S.; Fontecave, M.; Artero, V. Molecular Engineering of a Cobalt-based Electrocatalytic Nano-Material for H<sub>2</sub> Evolution under Fully Aqueous Conditions. *Nat. Chem.* **2013**, *5*, 48–53.
- (33) (a) Muresan, N. M.; Willkomm, J.; Mersch, D.; Vaynzof, Y.; Reiser, E. Immobilization of a Molecular Cobaloxime Catalyst for Hydrogen Evolution on a Mesoporous Metal Oxide Electrode. *Angew. Chem., Int. Ed.* **2012**, *51*, 12749–12753. (b) Gerli, A.; Sabat, M.; Marzilli, L. G. Lariat-Type-B<sub>12</sub> Model Complexes 0.1. New Pendant Methylpyridyl Costa-Type Organocobalt Complexes Provide Insight into the Role of the Axial Ligand in Butterfly Bending and Redox Properties. *J. Am. Chem. Soc.* **1992**, *114*, 6711–6718. (c) Reynal, A.; Willkomm, J.; Muresan, N. M.; Lakadamyali, F.; Planells, M.; Reiser, E.; Durrant, J. R. Distance dependent charge separation and recombination in semiconductor/molecular catalyst systems for water splitting. *Chem. Commun.* **2014**, *50*, 12768–12771.
- (34) Sletten, E. M.; Bertozzi, C. R. From Mechanism to Mouse: A Tale of Two Bioorthogonal Reactions. *Acc. Chem. Res.* **2011**, *44*, 666–676.
- (35) (a) Le Goff, A.; Artero, V.; Metayé, R.; Moggia, F.; Jusselme, B.; Razavet, M.; Tran, P. D.; Palacin, S.; Fontecave, M. Immobilization of FeFe hydrogenase mimics onto carbon and gold electrodes by controlled aryldiazonium salt reduction: An electrochemical, XPS and ATR-IR study. *Int. J. Hydrogen Energy* **2010**, *35*, 10719–10724. (b) Le Goff, A.; Moggia, F.; Debou, N.; Jegou, P.; Artero, V.; Fontecave, M.; Jusselme, B.; Palacin, S. Facile and tunable functionalization of carbon nanotube electrodes with ferrocene by covalent coupling and pi-stacking interactions and their relevance to glucose bio-sensing. *J. Electroanal. Chem.* **2010**, *641*, 57–63.
- (36) Thus excluding the formation of the catalytically active H<sub>2</sub>-CoCat under turnover conditions.
- (37) (a) Le Goff, A.; Artero, V.; Jusselme, B.; Tran, P. D.; Guillet, N.; Metayé, R.; Fihri, A.; Palacin, S.; Fontecave, M. From Hydrogenases to Noble Metal-Free Catalytic Nanomaterials for H<sub>2</sub> Production and Uptake. *Science* **2009**, *326*, 1384–1387. (b) Tran, P. D.; Le Goff, A.; Heidkamp, J.; Jusselme, B.; Guillet, N.; Palacin, S.; Dau, H.; Fontecave, M.; Artero, V. Noncovalent Modification of Carbon Nanotubes with Pyrene-Functionalized Nickel Complexes: Carbon Monoxide Tolerant Catalysts for Hydrogen Evolution and Uptake. *Angew. Chem., Int. Ed.* **2011**, *50*, 1371–1374.
- (38) Hulley, E. B.; Wolczanski, P. T.; Lobkovsky, E. B. Carbon–Carbon Bond Formation from Azaallyl and Imine Couplings about Metal–Metal Bonds. *J. Am. Chem. Soc.* **2011**, *133*, 18058–18061.
- (39) (a) Shi, S.; Bakac, A.; Espenson, J. H. Reduction-Induced Cleavage of the Cobalt Carbon Bond in Macrocyclic Organocobalt Complexes. *Inorg. Chem.* **1991**, *30*, 3410–3414. (b) Simandi, L. I.; Budo-Zahonyi, E.; Szeverenyi, Z. Effect of Strong Base on the Activation of Molecular Hydrogen by Pyridinebis-(dimethylglyoximate)cobalt(II). *Inorg. Nucl. Chem. Lett.* **1976**, *12*, 237–241. (c) Simandi, L. I.; Szeverenyi, Z.; Budozahonyi, E. Activation of Molecular-Hydrogen by Cobaloxime(II) Derivatives. *Inorg. Nucl. Chem. Lett.* **1975**, *11*, 773–777.
- (40) Tran, P. D.; Artero, V.; Fontecave, M. Water electrolysis and photoelectrolysis on electrodes engineered using biological and bio-inspired molecular systems. *Energy Environ. Sci.* **2010**, *3*, 727–747.

(41) Berben, L. A.; Peters, J. C. Hydrogen evolution by cobalt tetraimine catalysts adsorbed on electrode surfaces. *Chem. Commun.* **2010**, *46*, 398–400.

(42) Scherer, M. R. J.; Muresan, N. M.; Steiner, U.; Reisner, E. RYB tri-colour electrochromism based on a molecular cobaloxime. *Chem. Commun.* **2013**, *49*, 10453–10455.

(43) Zhang, P.; Jacques, P.-A.; Chavarot-Kerlidou, M.; Wang, M.; Sun, L.; Fontecave, M.; Artero, V. Phosphine Coordination to a Cobalt Diimine–Dioxime Catalyst Increases Stability during Light-Driven H<sub>2</sub> Production. *Inorg. Chem.* **2012**, *51*, 2115–2120.

(44) Dempsey, J. L.; Winkler, J. R.; Gray, H. B. Mechanism of H<sub>2</sub> Evolution by a Photogenerated Hydridocobaloxime. *J. Am. Chem. Soc.* **2010**, *132*, 16774–16776.

(45) Bhattacharjee, A.; Chavarot-Kerlidou, M.; Dempsey, J. L.; Gray, H. B.; Fujita, E.; Muckerman, J. T.; Fontecave, M.; Artero, V.; Arantes, G. M.; Field, M. J. Theoretical Modeling of Low-Energy Electronic Absorption Bands in Reduced Cobaloximes. *ChemPhysChem* **2014**, *15*, 2951–2958.

(46) Probst, B.; Guttentag, M.; Rodenberg, A.; Hamm, P.; Alberto, R. Photocatalytic H<sub>2</sub> Production from Water with Rhenium and Cobalt Complexes. *Inorg. Chem.* **2011**, *50*, 3404–3412.

(47) Oberholzer, M.; Probst, B.; Bernasconi, D.; Spingler, B.; Alberto, R. Photosensitizing Properties of Alkynylrhenium(I) Complexes [Re(–C≡C–R)(CO)<sub>3</sub>(N∩N)] (N∩N = 2,2'-bipy, phen) for H<sub>2</sub> Production. *Eur. J. Inorg. Chem.* **2014**, *2014*, 3002–3009.

(48) (a) Guttentag, M.; Rodenberg, A.; Kopelent, R.; Probst, B.; Buchwalder, C.; Brandstatter, M.; Hamm, P.; Alberto, R. Photocatalytic H<sub>2</sub> Production with a Rhenium/Cobalt System in Water under Acidic Conditions. *Eur. J. Inorg. Chem.* **2012**, *2012*, 59–64.

(b) Varma, S.; Castillo, C. E.; Stoll, T.; Fortage, J.; Blackman, A. G.; Molton, F.; Deronzier, A.; Collomb, M. N. Efficient photocatalytic hydrogen production in water using a cobalt(III) tetraaza-macrocyclic catalyst: electrochemical generation of the low-valent Co(I) species and its reactivity toward proton reduction. *Phys. Chem. Chem. Phys.* **2013**, *15*, 17544–17552.